Possible role of phase segregation in the disagreement between the metal-insulator and ferromagnetic transition temperatures in some colossal magnetoresistance compounds

Hirotoshi Terashita and J. J. Neumeier

Department of Physics, Florida Atlantic University, Boca Raton, Florida 33431-0991

The isovalent substitution of Gd for La in $La_{0.7}Ca_{0.3}MnO_3$ lowers the paramagnetic-ferromagnetic transition temperature T_c and metal-insulator transition temperature T_{MI} with a substantial increase in the electrical resistivity ρ. Reduction of the ferromagnetic saturation moment M (5 K) below that expected for complete ferromagnetic alignment of the Mn magnetic moments occurs and T_{MI} is significantly lower than T_c for $x > 0.2$. The observations are consistent with the existence of a granular mixture of ferromagnetic/conducting La-Ca-Mn-O and ferrimagnetic/insulating Gd-Ca-Mn-O. The ionic radius of the substituted rare-earth ion is found to be an important factor in determining whether or not granular behavior occurs. The results provide insight into why $T_c \neq T_{MI}$ in some colossal magnetoresistance oxides.

I. INTRODUCTION

The charge, lattice, and magnetic degrees of freedom in the manganese oxides exhibit an unusually strong coupling which leads to a magnetoresistance effect referred to as colossal magnetoresistance (CMR).[1,2] Recently the occurrence of magnetic and electronic phase segregation has become a topic of intense interest[3] in the study of CMR. The observation of real-space ordering of charge in manganese, nickel, and copper oxides[4,5] and computational studies reveal electronic/magnetic phase segregation in the manganese oxides whereby ferromagnetic and antiferromagnetic regions coexist or ferromagnetic clusters coexist within a paramagnetic background in otherwise compositionally homogeneous systems.[3,6] These results are supported by various experiments which display ferromagnetic cluster formation.[7-9] The strong competition between ferromagnetism and other coexisting phases is expected to strongly influence the magnetoresistivity,[3] thus the phase segregation scenario provides a theoretical view of CMR that is alternative to the local mean-field approach which neglects charge inhomogeneity.[3]

Experiments show that the conduction electron mobility and ferromagnetic transition temperature T_c are determined not only by the concentration of conduction electrons,[2] but also by the transfer integral between Mn^{3+} and Mn^{4+} ions which depends on the Mn-O-Mn bond angle.[1,10] The bond angle can be varied through chemical substitutions[1,10] or the application of high pressure.[10-12] In the case of the herein investigated $Gd_{0.7}Ca_{0.3}MnO_3$ and $La_{0.7}Ca_{0.3}MnO_3$ solid solutions, substitution of the smaller rare-earth Gd ion for La should decrease the Mn-O-Mn bond angle and decrease T_c. While $La_{0.7}Ca_{0.3}MnO_3$ is the well-known ferromagnetic CMR material, $Gd_{0.7}Ca_{0.3}MnO_3$ displays a complex magnetic behavior.[13-15] Two ferromagnetic lattices, one associated with the Gd moments and the other with the Mn moments, create a ferrimagnetic state below 80 K (Ref. 13) in $Gd_{0.67}Ca_{0.33}MnO_3$ (assumed here as identical to $Gd_{0.7}Ca_{0.3}MnO_3$). $Gd_{0.67}Ca_{0.33}MnO_3$ is a very poor conductor[13-15] with $\rho(40\ K) = 26$ GΩ cm. In typical CMR

systems T_c agrees with the metal-insulator transition temperature T_{MI}. Our study of $(La_{1-x}Gd_x)_{0.7}Ca_{0.3}MnO_3$ reveals that Gd substitution for La systematically reduces T_c and T_{MI} and increases ρ. At concentrations $x > 0.2$, T_c is no longer equal to T_{MI} and the low-temperature ferromagnetic saturation moment is decreased from the expected value of $3.7\mu_B$/Mn ion, where μ_B is the Bohr magneton. Our observations suggest a mixture of two independent electronic phases consisting of electrically conducting and ferromagnetic La-Ca-Mn-O with insulating and ferrimagnetic Gd-Ca-Mn-O and results in physical behavior comparable to that of granular metals consisting of a metal interspersed with insulating material. This phase segregation may be related to the electronic phase segregation[6] mentioned above, although here the doped electron concentration is expected to be homogeneous. Our findings, considered with results from the literature, indicate that granular behavior is common in the $LaMnO_3$ system when the ionic radius of the substituted rare-earth ion is smaller than that of La by 0.1 Å or more.

II. EXPERIMENTAL DETAILS

Polycrystalline samples $(La_{1-x}Gd_x)_{0.7}Ca_{0.3}MnO_3$ ($0 \leq x \leq 0.3$) were prepared from stoichiometric amounts of high-purity (99.99% or higher) La_2O_3 (dried at 600 °C), Gd_2O_3, $CaCO_3$, and MnO_2 powders. These were mixed for 20 min followed by reaction for 20 h at 1200 °C. The specimens were reground for 20 min, reacted for 20 h at 1200 °C, reground for 20 min, reacted for 20 h at 1300 °C. This step was repeated four additional times, followed by regrinding for 20 min, pressing into pellets, reaction for 17 h at 1300 °C and cooling at a rate of 1.5 °C/min for $0 \leq x \leq 0.3$ specimens. The specimens $0.4 \leq x \leq 1$ were prepared similarly with a maximum reaction temperature of 1375 °C. Another set of samples in the range $0 < x \leq 0.3$ were made with two less grindings, and reaction to maximum temperatures of 1300 and 1375 °C; they displayed broader ferromagnetic transitions, but were otherwise comparable to the specimens prepared as outlined above. The extra intermediate grindings, rather than reaction temperature, improves the specimen homogeneity providing sharper magnetic and metal-insulator
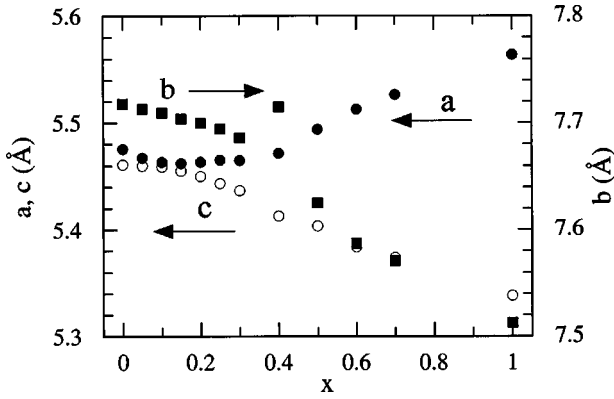
FIG. 1. Lattice constants at $T = 300$ K for $(La_{1-x}Gd_x)_{0.7}Ca_{0.3}MnO_3$. Solid circles, solid squares, and open circles represent a, b, and c, respectively.

transitions. The resistivity was measured during cooling by a four-probe dc technique. The magnetization was measured with a commercial dc superconducting quantum interference device magnetometer; the specimens were cooled in zero field and measured as the temperature was increased.

III. RESULTS

A. Structural results

Powder x-ray diffraction showed all specimens are single phase. Rietveld refinements of structural data were conducted with the GSAS program[16] revealing an orthorhombic perovskite structure with space group *Pnma* as reported previously.[13] Figure 1 shows the lattice parameters for $(La_{1-x}Gd_x)_{0.7}Ca_{0.3}MnO_3$ with $0 \leqslant x \leqslant 1$ at 300 K. Due to the small ionic size of Gd relative to La and Ca, a, b, and c decrease slightly as Gd is substituted for La in the region $0 \leqslant x \leqslant 0.2$. In the region $0.25 \leqslant x \leqslant 1$, b and c continue to decrease while a increases leading to a more pronounced orthorhombic distortion.

B. Magnetic properties

Figure 2(a) shows the magnetization M versus temperature T for $(La_{1-x}Gd_x)_{0.7}Ca_{0.3}MnO_3$ with $0 \leqslant x \leqslant 0.3$ in a magnetic field $H = 4$ kOe. This magnetic field is large enough to saturate the magnetization of $La_{0.7}Ca_{0.3}MnO_3$ at 5 K. The ferromagnetic transition temperature T_c decreases with x and $M(T)$ below T_c is significantly broader for specimens with $x \geqslant 0.2$. Considering only the Mn magnetic moments, taking the orbital angular momentum $L = 0$, and assuming that all spins in unfilled Mn shells are ferromagnetically aligned, the total magnetic moment M_0 at $T = 0$ K for $La_{0.7}Ca_{0.3}MnO_3$ is estimated as $M_0 = gS\mu_B$; in this relation $g = 2$ and S is the average spin on the Mn ion. The ratio $Mn^{3+}/Mn^{4+} = \frac{7}{3}$ leads to $S = 1.85$ and $M_0 = 3.7\mu_B$. This value agrees well with observed saturation moments M_{sat} (5 K), determined from the inflection point in $M(H)$ below 5 kOe, for $0 \leqslant x \leqslant 0.2$ displayed in Fig. 2(a) and Table I. For $x = 0.25$ and 0.3, M_{sat} (5 K) is significantly below the value $M_0 = 3.7\mu_B$ indicating either incomplete fer-
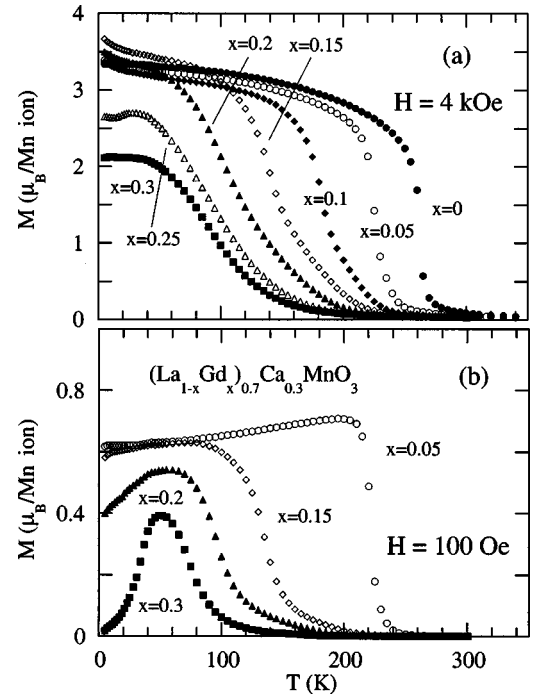
FIG. 2. (a) Temperature dependence of the magnetization M in applied magnetic field $H = 4$ kOe for $(La_{1-x}Gd_x)_{0.7}Ca_{0.3}MnO_3$ ($0 \leqslant x \leqslant 0.3$). (b) M versus T at $H = 100$ Oe for $x = 0.05$, 0.15, 0.2, and 0.3.

romagnetic Mn moment alignment or the existence of a second magnetic phase with a smaller saturation moment.

In Fig. 3(a) M versus T is presented for $(La_{1-x}Gd_x)_{0.7}Ca_{0.3}MnO_3$ with $x = 0.4$, 0.6, 0.7, and 1. Unlike what is seen in Fig. 2(a), typical ferromagnetic behavior is not observed. The magnetization remains well below the expected value $M_0 = 3.7\mu_B$ at all temperatures. The peak near 30 K for the $x = 0.4$ specimen moves to slightly higher temperature with increase of x. This peak results from ferrimagnetic (FIM) order whereby the Gd ions align antiferromagnetically with regard to the Mn ferromagnetic lattice, as previously discussed for $Gd_{0.67}Ca_{0.33}MnO_3$.[13] Low-field measurements were carried out to highlight the peak in M versus T. The magnetization measurements for $x = 1$ reveal behavior similar to that reported earlier[13] with a peak in $M(T)$ near 55 K, a minimum in M near 20 K and hysteresis in M (5 K) versus H as shown in Fig. 3(b) and the inset thereof. A similar peak in $M(T)$ is observed in Fig. 2 near 50 K for specimens with $x \geqslant 0.2$ while no peak occurs for specimens with $x \leqslant 0.15$. These data suggest that FIM Gd-Ca-Mn-O regions exist in the samples for compositions $x > 0.2$.

The magnetization M (5 K) versus H is displayed in the inset of Fig. 3(a) for selected specimens. The measured saturation moments at 5 K, M_{sat} (5 K), for all specimens are presented in Table I. Saturation of M occurs near 3 kOe for $x \leqslant 0.1$ with M (5 K) attaining the M_0 value expected for full ferromagnetic Mn moment alignment. The specimens with $x > 0$ display an additional linear in H component for M above ≈ 3 kOe causing $M(H)$ to rise above that observed for $x = 0$, a behavior attributable to the presence of paramagnetic Gd moments. This can be seen if the expected paramagnetic

TABLE I. Values of the average A-site ion ionic radius, $\langle r_A \rangle$, metal-insulator transition temperature, T_{MI}, and ferromagnetic transition temperature T_c, the electrical resistivity at 5 K, ρ (5 K), the electrical resistivity at T_{MI}, ρ_{max} and the saturated magnetization values M_{sat} (5 K) for $(La_{1-x}Gd_x)_{0.7}Ca_{0.3}MnO_3$ specimens.

x	0	0.05	0.10	0.15	0.20	0.25	0.30
$\langle r_A \rangle$ (Å)[a]	1.148	1.144	1.141	1.137	1.133	1.129	1.126
T_{MI} (K)[b]	265	238	200	161	120	89	50
T_c (K)[c]	268	237	204	177	168	151	138
ρ (5 K) (Ω cm)	4.5×10^{-3}	3.8×10^{-3}	6.8×10^{-3}	2.1×10^{-2}	3.9×10^{-2}	0.17	2.5×10^4
ρ_{max} (Ω cm)	4.6×10^{-2}	0.10	0.35	3.1	25	410	2.3×10^5
M_{sat} (5 K)	3.38	3.73	3.45	3.71	3.50	2.83	2.11

[a]Ionic radii for eight-coordinated La^{3+}, Gd^{3+}, and Ca^{2+} ions from Ref. 21 were used to calculate $\langle r_A \rangle$.
[b]T_{MI} is determined as the temperature where $\rho = \rho_{max}$.
[c]T_c was determined as the intersection point of two linear lines drawn through the data above and below the temperature region near the ferromagnetic transition.

behavior, calculated with the Brillouin function for Gd with total angular momentum $J = \frac{7}{2}$,[17] is subtracted from the data as illustrated for $x=0.15$ by the dashed line in the inset of Fig. 3(a). This correction leads to a typical ferromagnetic (FM) response for $M(H)$ above 3 kOe. A correction of this type is successful only for $x<0.20$ suggesting that Gd-Gd magnetic interactions play a role at higher doping levels.

Incomplete ferromagnetic order similar to that revealed in Figs. 2 and 3 is often ascribed to canting of the ferromagnetic moments which is expected to occur within the double exchange (DE) model[18] for Ca doping levels other than that

FIG. 3. (a) Temperature dependence of the magnetization M for $(La_{1-x}Gd_x)_{0.7}Ca_{0.3}MnO_3$ ($0.4 \leqslant x \leqslant 1$) in $H=4$ kOe. Field dependence of M at $T=5$ K for $x=0.15$, 0.4, and 0.7 is presented in the inset; the dashed line is for $x=0.15$ after correction for paramagnetic Gd moments. (b) Temperature dependence of M for $x=0.4$, 0.6, 0.7, and 1 in $H=100$ Oe using identical symbols as in (a). The hysteresis loop at $T=5$ K for $x=1$ is displayed in the inset.

considered herein and is probably not of major importance for the Gd doped specimens. Rather than canting, the magnetic measurements suggest a simple two-lattice model for the low-temperature magnetic properties of these specimens. In the regime $x<0.20$ one magnetic lattice is due to the paramagnetic Gd moments and the second is that formed by the ferromagnetic Mn ions. At Gd concentrations $x \geqslant 0.20$, the increased density of Gd ions leads to the formation of Gd-Ca-Mn-O FIM regions which cause a reduction in M_{sat} (5 K) and the development of a peak in $M(T)$. For the region $0.20 \leqslant x<1$, FM and FIM regions coexist, this phase segregation becomes most apparent in the region $0.4 \leqslant x \leqslant 0.7$.

This picture is supported by a simple phenomenological model involving the contribution of FM $(La_{0.7}Ca_{0.3}MnO_3)_{1-x}$ and FIM $(Gd_{0.7}Ca_{0.3}MnO_3)_x$ clusters in $(La_{1-x}Gd_x)_{0.7}Ca_{0.3}MnO_3$. The FM $(La_{0.7}Ca_{0.3}MnO_3)_{1-x}$ clusters possess a net magnetic moment $3.7\mu_B$ as explained above. The FIM $(La_{0.7}Gd_{0.3}MnO_3)_x$ clusters contain Mn and Gd ions ordered ferrimagnetically resulting in a net magnetic saturation moment per Mn ion given by $M=[2\times0.7\times\frac{7}{2}-3.7]\mu_B=1.2\mu_B$ at $T=0$ K.[13] Two possible alignments of the FM and FIM clusters with regard to one another exist: (i) the net moments from the FM and FIM clusters are aligned parallel or (ii) antiparallel. For case (i), the total magnetization per Mn ion is estimated as $M=[3.7(1-x)+1.2(x)]\mu_B$ (dashed line in Fig. 4). For case (ii), the total magnetization per Mn ion is estimated as $M=[3.7(1-x)-1.2(x)]\mu_B$ (solid line in Fig. 4). Our data in Fig. 4, with M_{sat} (5 K) determined as the inflection point in $M(H)$, agree well with case (ii) thereby providing further support for the proposed two-lattice model.

C. Electrical resistivity

The electrical resistivity $\rho(T)$ for $(La_{1-x}Gd_x)_{0.7}Ca_{0.3}MnO_3$ with $0 \leqslant x \leqslant 0.3$ is shown in Fig. 5. Gd substitution dramatically alters ρ and decreases T_{MI} in a systematic fashion. The electrical resistivity beyond $x=0.3$ is too high for measurement with our experimental apparatus. Although ρ (300 K) is only weakly affected by Gd substitution, the peak in ρ increases by nearly six orders of magnitude in the doping range illustrated in Fig. 5. A strong
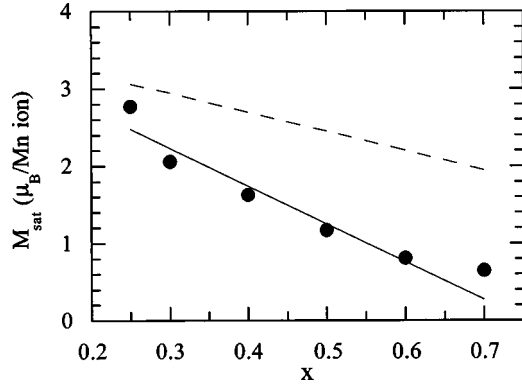
FIG. 4. The saturation moment M_{sat} (5 K) is plotted (solid circles) as a function of x for $(La_{1-x}Gd_x)_{0.7}Ca_{0.3}MnO_3$. The dashed line and solid lines represent a phenomenological model with the net magnetic moments from the FM and FIM components aligned parallel and antiparallel, respectively.

correlation exists between the electrical transport and magnetic properties as illustrated in the inset of Fig. 5 where M_{sat} (5 K) and ρ (5 K) are plotted versus x on a log scale; for $x > 0.2$ the sharp increase of ρ (5 K) corresponds well with the decrease of M_{sat}. At a doping level of $x = 0.25$, the resistivity at 5 K is more than two orders of magnitude larger than for $x = 0$ while the resistivity at 5 K for $(La_{0.75}Pr_{0.25})_{0.7}Ca_{0.3}MnO_3$ is almost the same as that for $La_{0.7}Ca_{0.3}MnO_3$ (Ref. 1) indicating that Gd substitution is significantly more efficient at destroying the charge carrier transport at low temperature than is Pr substitution. It is interesting that T_{MI} corresponds well with T_c only for $x < 0.2$ (see Table I). In all other cases T_{MI} is significantly below T_c. These observations suggest that the degradation of ferromagnetic and electrical properties in this system are intimately related. Similar behavior arises in substitutions of the form $(La_{1-x}Y_x)_{0.7}Ca_{0.3}MnO_3$ and $(La_{0.8}Gd_{0.2})_{0.72}Sr_{0.28}MnO_3$.[19,20]

IV. DISCUSSION

In order to understand the observations above, the structural effects of Gd doping should be considered. Substituting
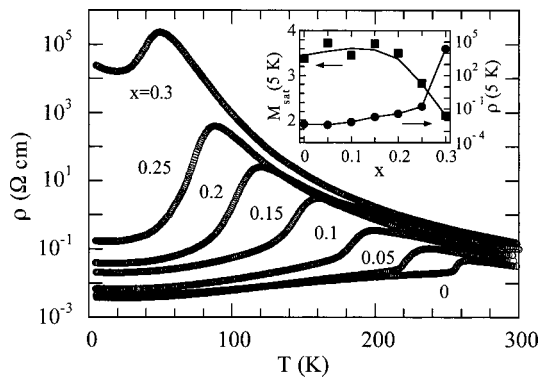
FIG. 5. Temperature dependence of electrical resistivity ρ for $(La_{1-x}Gd_x)_{0.7}Ca_{0.3}MnO_3$ in the range $0 \leq x \leq 0.3$ plotted on a logarithmic scale. In the inset, the magnetic saturation moment M_{sat} (5 K) is plotted as the solid squares versus x and the ρ (5 K) is plotted on a logarithmic scale as the solid circles. The lines are drawn as guides to the eye.
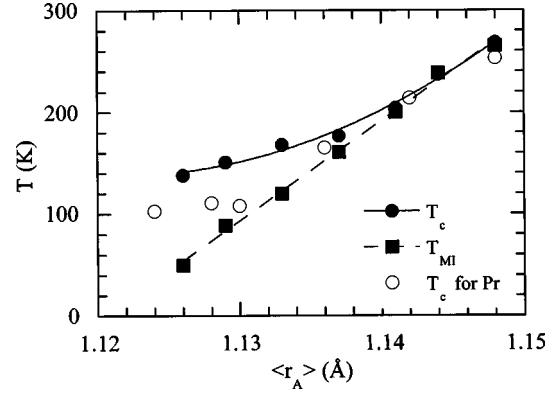
FIG. 6. Ferromagnetic transition temperature T_c (solid circles) and metal insulator transition temperature T_{MI} (solid squares) versus average A-site ionic radius $\langle r_A \rangle$ for $x \leq 0.3$. Selected data for T_c were obtained from the literature (Refs. 1 and 12) (open circles) illustrating specimens where $T_c = T_{MI}$. Lines are drawn as guides to the eye.

La with smaller rare-earth ions is known to decrease the Mn-O-Mn bond angle leading to a decrease of T_c; the average A-site ionic radius $\langle r_A \rangle$ can also be used to parameterize this decrease of T_c.[1,12] Values of $\langle r_A \rangle$ were calculated using the ionic radii for eight-coordinated La^{3+}, Gd^{3+}, and Ca^{2+} ions,[21] these values are presented in Table I. A plot of T_c and T_{MI} versus $\langle r_A \rangle$ $(x \leq 0.3)$ is presented in Fig. 6 revealing a decrease in T_c that is weaker than that of T_{MI}. These results suggest that the electrical and magnetic properties are less weakly coupled below $\langle r_A \rangle \approx 1.138$ Å. T_c values for $(La_{1-x}Pr_x)_{0.7}Ca_{0.3}MnO_3$ from Hwang and co-workers,[1,12] for which full ferromagnetic order are observed, are shown for comparison (open circles). Interestingly, these data agree quite well with our T_{MI} values for $0 \leq x \leq 0.2$. A noteworthy aspect is the physical properties of $Gd_{0.7}Ca_{0.3}MnO_3$ and $Pr_{0.7}Ca_{0.3}MnO_3$. $Pr_{0.7}Ca_{0.3}MnO_3$ is insulating at 50 K with ρ (50 K) ≈ 1 MΩ cm and a significant magnetoresistance, moderate hydrostatic pressure (pressure increases the Mn-O-Mn bond angle toward 180°) of about 1 GPa results in a metal-insulator transition typical of CMR compounds.[12,22] This observation suggests that, from a structural standpoint $Pr_{0.7}Ca_{0.3}MnO_3$ is near to being a CMR compound. On the other hand, $Gd_{0.67}Ca_{0.33}MnO_3$, has an electrical resistivity at 40 K of 26 GΩ cm and no significant magnetoresistance[13–15] suggesting that it is further from the metal-insulator/CMR phase boundary than $Pr_{0.7}Ca_{0.3}MnO_3$.

Careful consideration of the ionic radii of the dopants is quite revealing with regard to the observed behavior. From Ref. 21 the ionic radii for the ions used in this and other studies were found to be: La^{3+} (1.160 Å), Pr^{3+} (1.126 Å), Ca^{2+} (1.120 Å), Gd^{3+} (1.053 Å), and Y^{3+} (1.019 Å). The discussion above revealed that substitutions of Pr for La retain the $T_c = T_{MI}$ relationship, result in a strong depression of T_c, and less pronounced enhancement of ρ (5 K); in this case the ionic radii for La^{3+} and Pr^{3+} differ by 0.034 Å. Samples of the form $(La_{0.76}Sm_{0.24})_{0.7}Sr_{0.3}MnO_3$ also exhibit $T_c = T_{MI}$; here, the ionic radii of La^{3+} and Sm^{3+} (1.079 Å) differ by 0.081 Å.[20,25] On the other hand, substitutions of Y for La (Refs. 1 and 19) or Gd for La result in $T_c \neq T_{MI}$, a less

pronounced depression of T_c, and a reduction of the ferromagnetic saturation moment; in these cases, the ionic radii differ by 0.141 and 0.107 Å, respectively. Comparison of these substitutions indicates that substituted ions with ionic radii smaller than that of La^{3+} by 0.1 Å or more have a weaker influence on the magnetic transition temperature, a dramatic influence on the electrical resistivity, and lead to incomplete ferromagnetic order.

Noting the poor electrical conductivity of $Gd_{0.7}Ca_{0.3}MnO_3$ (Refs. 13–15) in comparison to $La_{0.7}Ca_{0.3}MnO_3$, Gd-Ca-Mn-O islands are likely to localize charge carriers, increase the bulk electrical resistivity and, at a high enough concentration, eventually lead to percolative conduction where conductivity takes place via tunneling through Gd-Ca-Mn-O regions from one La-Ca-Mn-O region to another. In addition, the region of the La-Ca-Mn-O matrix adjacent to a Gd-Ca-Mn-O island is likely to be strongly distorted, due to the small Gd ionic size, which will affect the properties of the matrix. Local changes in the Jahn-Teller distortion could also play a role. The solid solution of $Gd_{0.7}Ca_{0.3}MnO_3$ and $La_{0.7}Ca_{0.3}MnO_3$ can be compared to mixtures of conducting and nonconducting materials in sputtered thin films of Ni or Al mixed with SiO_2 which have been studied extensively and are referred to as granular metals.[23,24] As x increases beyond a certain limit, the percolation threshold is reached, causing a strong increase in the bulk resistivity. Studies of granular metals, such as Al or Ni thin films mixed with SiO_2 reveal a dependence of ρ on the volume fraction of SiO_2 (Refs. 23 and 24) that is reminiscent of what is displayed in the inset of Fig. 5. For manganese oxides, the situation is more complicated than that of simple granular metals because of the complex $\rho(T)$ dependence for CMR compounds, but the analogy between these two systems makes physical sense in lieu of the magnetic and electrical transport properties revealed in this study. Rietveld refinements of the x-ray data using the two distinct phases $La_{0.7}Ca_{0.3}MnO_3$ and $La_{0.7}Gd_{0.3}MnO_3$ in appropriate ratios, as a structural test of this granular picture, could not produce converging fits suggesting that a crystallographically single-phase solid solution $(La_{1-x}Gd_x)_{0.7}Ca_{0.3}MnO_3$ exists. Therefore our observations indicate the existence of two distinct magnetic/electronic phases in a crystallographically single-phase system.

From the discussion above, $x \approx 0.2$ seems to be the critical value above which the effects of Gd-Ca-Mn-O islands make their presence apparent. The following simple explanation is offered to understand the origin of this critical concentration. Each A-site ion possesses six nearest-neighbor A-site ions thus forming a group of 7 which we call a seven cluster. Consider for simplicity that the A-site ions are made up of two different elements, element X and Z with element X making up the majority. When element Z is at a concentration of $(\frac{1}{7}) \approx 14\%$, under ideal homogeneity conditions every seven cluster possesses an ion of element Z. At doping levels above this, islands consisting of three or more adjacent $ZMnO_3$ unit cells must form. Furthermore, substitution of one X ion with a Z ion affects all eight Mn ions which are

immediate neighbors, therefore, under ideal homogeneity conditions a Z ion concentration of 12.5% would, to some extent, affect all Mn ions. In the case of the Gd doped samples considered herein, the concentration $x = 0.2$ corresponds to an A-site Gd concentration of 14%, the borderline above which formation of Gd-Ca-Mn-O islands is certain. These simple considerations provide a physical basis for our observation of FIM behavior attributable to Gd-Ca-Mn-O islands at doping levels $x \geq 0.20$ and for the onset of percolative conduction with x below the percolation limit.

V. CONCLUSIONS

In the low x regime $(x < 0.2)$ T_c of $(La_{1-x}Gd_x)_{0.7}Ca_{0.3}MnO_3$ is systematically reduced with $\langle r_A \rangle$ because the Gd-Ca-Mn-O islands are dispersed in the FM La-Ca-Mn-O matrix with a high probability for the existence of a continuous conducting path and a low probability for the existence of larger FIM Gd-Ca-Mn-O islands which possess poor electrical conductivity; the Gd ions behave paramagnetically in this range. For $x \geq 0.2$, Gd doping increases the fraction of FIM phase leading to a rapid increase of ρ (5 K) and $T_c \neq T_{MI}$ as well as the development of Gd-Gd magnetic interactions. The mixture of ferromagnetic/conducting La-Ca-Mn-O with a large enough concentration $(x > 0.2)$ of ferrimagnetic/poorly conducting islands of Gd-Ca-Mn-O results in percolative conduction because conducting paths along Mn-O-Mn bonds are destroyed. Within this picture, the disagreement between T_c and T_{MI} occurs as a result of competition among the two electronic/magnetic phases. When ferromagnetism within the distorted La-Ca-Mn-O regions begins to set in at T_c, the electrical resistivity there starts to decrease while the electrical resistivity of the Gd-Ca-Mn-O regions continues to increase. Further reduction of temperature increases the magnetization and electrical conductivity in the La-Ca-Mn-O regions eventually providing a conducting path where ρ decreases with temperature. The likelihood that this type of phase segregation occurs may be enhanced by the natural tendency for electronic phase segregation[6–9] in CMR-related systems, although in the present case the doped electron concentration is expected to be homogeneous.

In summary, Gd substitution for La in $La_{0.7}Ca_{0.3}MnO_3$ leads to effects quite different than those observed for substitutions where the size of the substituted rare earth is closer to that of La. These results indicate the existence of a phase segregated mixture of ferromagnetic/conducting La-Ca-Mn-O and ferrimagnetic/insulating Gd-Ca-Mn-O. This behavior appears to be common if the rare-earth ionic radius of the substituted ion is 0.1 Å or more smaller than that of La.

[1] H. Y. Hwang, S.-W. Cheong, P. G. Radaelli, M. Marezio, and B. Batlogg, Phys. Rev. Lett. **75**, 914 (1995).

[2] P. Schiffer, A. P. Ramirez, W. Bao, and S.-W. Cheong, Phys. Rev. Lett. **75**, 3336 (1995).

[3] A. Moreo, S. Yunoki, and E. Dagotto, Science **283**, 2034 (1999).

[4] W. Bao, J. D. Axe, C. H. Chen, and S.-W. Cheong, Phys. Rev. Lett. **78**, 543 (1997).

[5] C. H. Chen, S.-W. Cheong, and A. S. Cooper, Phys. Rev. Lett. **71**, 2461 (1993).

[6] E. Dagotto, S. Yunoki, A. L. Malvezzi, A. Moreo, J. Hu, S. Capponi, D. Poilblanc, and N. Furukawa, Phys. Rev. B **58**, 6414 (1998); A. Moreo, M. Mayr, A. Feiguin, S. Yunoki, and E. Dagotto, Phys. Rev. Lett. **84**, 5568 (2000).

[7] M. Uehara, S. Mori, C. H. Chen, and S.-W. Cheong, Nature (London) **399**, 560 (1999).

[8] M. Fäth, S. Freisem, A. A. Menovsky, Y. Tomioka, J. Aarts, and J. A. Mydosh, Science **285**, 1540 (1999).

[9] J. J. Neumeier and J. L. Cohn, Phys. Rev. B **61**, 14 319 (2000); M. M. Savosta, P. Novák, M. Marysko, Z. Jirák, J. Heijtmánek, J. Englich, J. Kohout, C. Martin, and B. Raveau, *ibid.* **62**, 9532 (2000).

[10] V. Laukhin, J. Fontcuberta, J. L. García-Muñoz, and X. Obradors, Phys. Rev. B **56**, R10 009 (1997).

[11] J. J. Neumeier, M. F. Hundley, J. D. Thompson, and R. H. Heffner, Phys. Rev. B **52**, R7006 (1995).

[12] H. Y. Hwang, T. T. M. Palstra, S.-W. Cheong, and B. Batlogg, Phys. Rev. B **52**, 15 046 (1995).

[13] G. J. Snyder, C. H. Booth, F. Bridges, R. Hiskes, S. DiCarolis, M. R. Beasley, and T. H. Geballe, Phys. Rev. B **55**, 6453 (1997).

[14] M. Rubinstein, D. J. Gillespie, J. E. Snyder, and T. M. Tritt, Phys. Rev. B **56**, 5412 (1997).

[15] M. Jaime, H. Hardner, M. B. Salamon, M. Rubinstein, P. Dorsey, and D. Emin, J. Appl. Phys. **81**, 4958 (1997).

[16] A. C. Larson and R. B. Van Dreele, *GSAS: The General Structure Analysis System* (Los Alamos National Laboratory, Los Alamos, NM, 1991).

[17] C. Kittel, in *Introduction to Solid State Physics* (Wiley, New York, 1986), p. 402.

[18] P.-G. de Gennes, Phys. Rev. **118**, 141 (1960).

[19] B. Martínez, J. Fontcuberta, A. Seffar, J. L. García-Muñoz, S. Piñol, and X. Obradors, Phys. Rev. B **54**, 10 001 (1996).

[20] J. R. Sun, G. H. Rao, J. K. Liang, and B. G. Shen, Appl. Phys. Lett. **71**, 3718 (1997).

[21] R. D. Shannon, Acta Crystallogr., Sect. A: Cryst. Phys., Diffr., Theor. Gen. Crystallogr. **A32**, 751 (1976).

[22] H. Yoshizawa, H. Kawano, Y. Tomioka, and Y. Tokura, Phys. Rev. B **52**, R13 145 (1995).

[23] R. M. White and T. H. Geballe, in *Long Range Order in Solids* (Academic, New York, 1979), p. 385.

[24] B. Abeles, P. Sheng, M. D. Coutts, and Y. Aire, Adv. Phys. **24**, 407 (1975).

[25] L. M. Rodriguez-Martinez and J. P. Attfield, Phys. Rev. B **54**, R15 622 (1996).